Comparison of Regional Myocardial Blood Flow and Perfusion in Dilated Cardiomyopathy and Left Bundle Branch Block: Role of Wall Thickening

Bernd Nowak, MD[1]; Christoph Stellbrink, MD[2]; Wolfgang M. Schaefer, MD, PhD[1]; Anil M. Sinha, MD, PhD[2]; Ole A. Breithardt, MD[2]; Hans-Juergen Kaiser, PhD[1]; Patrick Reinartz, MD[1]; Peter Hanrath, MD[2]; and Ulrich Buell, MD[1]

[1]Department of Nuclear Medicine, University Hospital, Aachen University of Technology, Aachen, Germany; and [2]Department of Internal Medicine I (Cardiology), University Hospital, Aachen University of Technology, Aachen, Germany

Heterogeneous perfusion in left bundle branch block (LBBB) has been demonstrated by ^{99m}Tc-methoxyisobutylisonitrile (MIBI) SPECT. Locally different contraction is also associated with LBBB. Quantitative analysis of myocardial SPECT is influenced by partial-volume effects depending on systolic wall thickening. Therefore, partial-volume effects may mimic perfusion heterogeneity in LBBB. **Methods:** Fifteen patients with nonischemic dilated cardiomyopathy and LBBB underwent resting ^{15}O-water PET, ^{99m}Tc-MIBI SPECT, and gated ^{18}F-FDG PET for analysis of wall thickening. Myocardial blood flow corrected for rate–pressure product (corrMBF), ^{99m}Tc-MIBI uptake, and wall thickening were determined in 4 left ventricular wall areas. In 14 patients, M-mode echocardiographic recordings were available for comparison. **Results:** Homogeneous distribution was found for corrMBF (1.09 ± 0.41 to 1.19 ± 0.31 mL × g^{-1} × min^{-1}). ^{99m}Tc-MIBI uptake and wall thickening were heterogeneous ($P < 0.0001$), with the lowest values septal (^{99m}Tc-MIBI, 65% ± 10%; wall thickening, 16% ± 14%) and the highest lateral (^{99m}Tc-MIBI, 84% ± 5%; wall thickening, 55% ± 17%). Similar relationships in systolic wall thickening were observed by M-mode echocardiography (anteroseptal, 20% ± 11%; posterolateral, 37% ± 18%; $P < 0.001$). **Conclusion:** Heterogeneity of ^{99m}Tc-MIBI uptake in LBBB corresponds to differences in wall thickening and does not reflect distribution of corrMBF. Supplementary analysis of wall thickening is recommended when assessing ^{99m}Tc-MIBI SPECT in LBBB.

Key Words: left bundle branch block; ^{15}O-water; ^{99m}Tc-methoxyisobutylisonitrile; wall thickening

J Nucl Med 2004; 45:414–418

Studies using ^{201}Tl or ^{99m}Tc-methoxyisobutylisonitrile (MIBI) with SPECT have demonstrated diminished septal perfusion in patients with complete left bundle branch block (LBBB) even in the absence of coronary artery disease (*1*,*2*). It has been postulated that a higher partial-volume effect and therefore a smaller count increase during systole because of reduced systolic wall thickening in the septum may mimic this hypoperfusion (*3*). PET with ^{15}O-labeled water (^{15}O-water) enables absolute quantification of myocardial blood flow (MBF) without being affected by the partial-volume effect through the introduction of perfusable tissue fraction (PTF) (*4*,*5*).

The aim of this study was to compare the regional distribution of left ventricular (LV) perfusion (measured with ^{99m}Tc-MIBI SPECT) and MBF (measured with ^{15}O-water PET) in patients with nonischemic dilated cardiomyopathy and LBBB. The focus of attention was the comparative assessment of regional myocardial wall thickening as estimated with gated ^{18}F-FDG PET and M-mode echocardiography.

MATERIALS AND METHODS

Patients

We investigated 15 patients with dilated cardiomyopathy and complete LBBB. Dilated cardiomyopathy was diagnosed by a reduced LV function in cine ventriculography with exclusion of coronary artery disease by coronary angiography. All patients were in heart failure of functional class III according to the New York Heart Association. Nuclear medicine studies were performed within 2 d. Patient characteristics are listed in Table 1.

^{15}O-Water PET

Two dynamic resting ^{15}O-water PET studies were started with the infusion of 700 MBq of ^{15}O-water. Each study used an ECAT EXACT 922/47 PET scanner (Siemens-CTI) and consisted of 24 frames (14 × 5 s, 3 × 10 s, 3 × 20 s, and 4 × 30 s). A 15-min period between the 2 studies was used for a transmission scan. Corrections for dead time, attenuation, scatter, and decay were

Received Aug. 5, 2003; revision accepted Oct. 13, 2003.

For correspondence or reprints contact: Bernd Nowak, MD, Department of Nuclear Medicine, University Hospital, Aachen University of Technology, Pauwelsstrasse 30, 52074 Aachen, Germany.

E-mail: bnowak@ukaachen.de

TABLE 1
Clinical Characteristics

Patient no.	Sex	Age (y)	QRS width (ms)	EDV (mL)	ESV (mL)	EF (%)	SBP (mm Hg)	DBP (mm Hg)	HR (min^{-1})	RPP (mm Hg × min^{-1})
1	F	50	164	631	591	6	110	75	76	8,360
2	F	64	180	346	308	11	100	65	72	7,200
3	M	60	170	134	77	43	120	75	74	8,880
4	F	79	150	123	85	30	210	100	72	15,120
5	M	33	180	591	555	6	98	63	90	8,820
6	F	71	145	292	254	13	105	70	88	9,240
7	F	63	158	109	61	44	130	70	76	9,880
8	F	62	160	189	117	38	135	70	66	8,910
9	F	66	140	223	164	26	163	100	61	9,943
10	F	77	160	150	116	23	135	88	82	11,070
11	M	40	160	447	410	8	115	73	86	9,890
12	F	65	200	258	200	22	150	88	63	9,450
13	M	50	180	334	262	22	115	73	52	5,980
14	F	68	170	273	220	20	100	50	66	6,600
15	M	68	160	300	234	22	150	88	66	9,900
Mean		61	165	293	244	22	129	77	73	9,281
± SD		13	15	160	164	12	30	14	11	2,116

EDV = end-diastolic volume; ESV = end-systolic volume; EF = ejection fraction; SBP = systolic blood pressure; DBP = diastolic blood pressure; HR = heart rate; RPP = rate–pressure product.

applied, and final images were reconstructed using filtered backprojection (Hann; cutoff, 0.4 Nyquist).

MBF derived from the ^{15}O-water PET studies was quantified using pixelwise modeling software (PMOD; University Hospital Zurich) (*6*). Because unprocessed ^{15}O-water PET images do not contain sufficient anatomic information for cardiac reorientation and myocardial segmentation, this software applies a factor analysis to the water data that allows reconstruction of 2 image sets: one representing myocardium and another representing blood pool. These factor images were then used for anatomic reference, that is, reorientation of the dynamic ^{15}O-water PET data and segmentation into the septal, anterior, lateral, and posterior walls, excluding the apex. Regions of interest were also drawn within the left and right ventricles to obtain blood time–activity curves as input function (*7*) and to correct for left and right ventricular spillover (*8*). Arterial and myocardial tissue time–activity curves were fitted to a single-tissue compartment tracer kinetic model (*4*,*9*) to give values of regional MBF (mL × g^{-1} × min^{-1}) free of the partial-volume effect through the introduction of PTF (*4*,*5*). Mean values for PTF were also obtained for each myocardial wall area.

Because MBF is closely related to the rate–pressure product (arterial systolic blood pressure × heart rate), MBF corrected for the rate–pressure product was calculated as corrected MBF (corrMBF = MBF/rate–pressure product × 10^4). Arterial blood pressure and heart rate were automatically monitored during the ^{15}O-water PET studies with a Dinamap 8100 monitor (Critikon Corp.). Results of both ^{15}O-water PET studies were averaged for every patient.

To measure the precision of the PET measurement in the single study session, we calculated the repeatability coefficient according to the method of Bland and Altman (*10*). This coefficient is defined as 1.96 × the SD of the differences and is recommended by the British Standards Institution (*11*). The repeatability coefficient is also given as a percentage of the average value of the 2 measurements.

^{99m}Tc-MIBI SPECT

Myocardial perfusion SPECT was performed 60 min after injection of 424 ± 17 MBq of ^{99m}Tc-MIBI, with a light meal taken by the patient after tracer application. Data were acquired with a dual-head γ-camera (Solus; Philips Medical Systems). Acquisition parameters and attenuation- and scatter-corrected reconstruction in a 128 × 128 matrix were described in detail elsewhere (*12*). Briefly, emission was performed in 3 independent energy windows: 140 ± 14 keV for emission, 120 ± 6 keV for scatter detection, and 90 ± 11 keV for backscatter detection. Datasets of windows 1 and 2 were processed to obtain a scatter-corrected dataset, which was then reconstructed using a Butterworth filter (cutoff, 0.7 Nyquist; order, 5; matrix, 128 × 128) and processed with the dataset of window 3 (filtered backprojection, ramp) to obtain a final segmented attenuation- and scatter-corrected transaxial dataset.

^{99m}Tc-MIBI images were reoriented according to the LV axes. A volumetric vector sampling method and a 25-segment model were used to display relative ^{99m}Tc-MIBI uptake as percentage of the segment with maximum activity. Mean ^{99m}Tc-MIBI uptake of the 4 LV wall areas (septal, anterior, lateral, and posterior)—each consisting of 6 segments—was calculated as the mean value of the respective 6 segments for every patient. The remaining apical segment was not included in the wall area analysis.

The transaxial resolution of the SPECT system was measured with a line source filled with ^{99m}Tc-pertechnetate. The line source was placed centrally in a physiologic thorax phantom (septal area of the simulated myocardium). The full width at half maximum was 24.9 mm after acquisition and reconstruction with the same parameters used in the patient studies.

Gated ^{18}F-FDG PET

All patients received 250 mg of acipimox 2 h before administration of ^{18}F-FDG and 50 g of glucose orally 1 h before. Gated ^{18}F-FDG PET (ECAT EXACT 922/47; Siemens-CTI) was per-

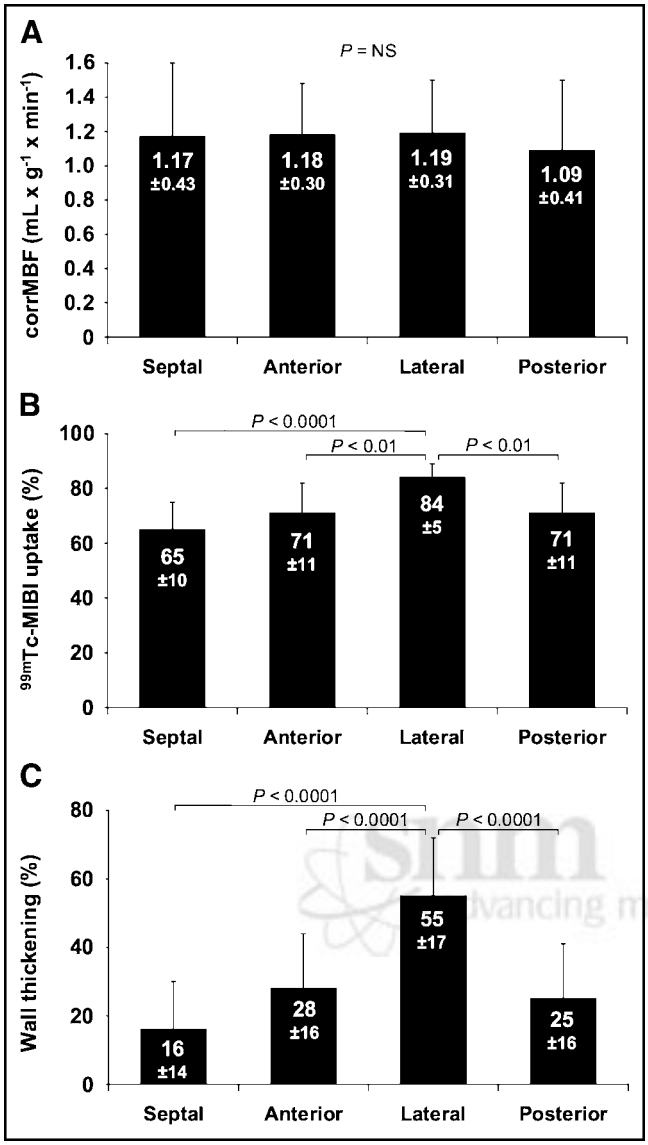

FIGURE 1. Distribution of LV corrMBF (A), ^{99m}Tc-MIBI uptake (B), and wall thickening (C) as determined by gated ^{18}F-FDG PET in 15 patients with LBBB without coronary artery disease.

formed 60 min after intravenous administration of 284 ± 30 MBq of ^{18}F-FDG with 8 gates per R-R interval. The acquisition time was 30 min for emission (2-dimensional mode) and 15 min for transmission (^{68}Ge/^{68}Ga rod sources). Attenuation-corrected gated images were reconstructed using an iterative algorithm (ordered-subsets expectation maximization, 16 subsets, 6 steps). The transaxial resolution of the PET system measured with the ^{18}F-FDG–filled line source in the thorax phantom was 10.9 mm in full width at half maximum.

The pixel size of gated ^{18}F-FDG images was changed to an isotropic 5.79 mm. These data were reoriented and analyzed for regional myocardial wall thickening and LV volumes using Quantitative Gated SPECT (Cedars-Sinai Medical Center) (*13*). Wall thickening was estimated in the 25-segment model and expressed as the percentage increase from end-diastolic myocardial thickness. Mean wall thickening of the 4 LV wall areas was calculated analogously to the determination of relative ^{99m}Tc-MIBI uptake values.

Echocardiography

Echocardiography recordings obtained within 1 mo before the nuclear medicine studies were available for 14 patients. Regional wall thickness for the anteroseptal and posterolateral walls was retrospectively measured from parasternal M-mode recordings without knowledge of the nuclear medicine results. End-diastole was identified by the onset of the QRS complex; end-systole was defined as the smallest LV diameter.

Statistical Analysis

Statistical analyses were performed with SPSS 11 software (SPSS Inc.). Data are expressed as mean ± SD. Differences of values between septal, anterior, lateral, and posterior myocardium were assessed with the 1-way ANOVA followed by a post hoc Bonferroni analysis. Parameters derived from echocardiography were tested using a *t* test for paired samples. $P < 0.05$ was considered significant.

RESULTS

At rest, corrMBF was homogeneously distributed in the LV myocardium, without significant differences between the respective wall areas (Fig. 1A). The mean PTF of the posterior wall (0.73 ± 0.11 g × mL^{-1}) was higher than that of the anterior wall (0.63 ± 0.06 g × mL^{-1}, $P < 0.05$) and that of the septum (0.59 ± 0.13 g × mL^{-1}, $P < 0.01$). PTF values of the lateral wall (0.68 ± 0.08 g × mL^{-1}), of the septum, and of the anterior wall did not differ significantly from one another. The repeatability coefficients for both ^{15}O-water PET measurements are shown in Table 2. The analysis revealed similar values for the septal, anterior, and posterior wall areas, with a slightly higher repeatability in the lateral wall.

In contrast to the corrMBF values, ^{99m}Tc-MIBI uptake proved to be heterogeneously distributed in the 4 LV wall areas ($P < 0.0001$; Fig. 1B). Mean ^{99m}Tc-MIBI uptake was significantly higher in the lateral wall (84% ± 5%) than in the remaining 3 wall areas. The lowest ^{99m}Tc-MIBI uptake was observed in the septum (65% ± 10%).

Analysis of regional wall thickening by gated ^{18}F-FDG PET demonstrated a significantly heterogeneous contraction

TABLE 2
Repeatability of MBF Measurements

Parameter	Repeatability coefficient: Absolute (mL × g^{-1} × min^{-1})	Repeatability coefficient: % of mean
Global		
MBF	0.15	15
corrMBF	0.44	38
Regional (MBF)		
Septal	0.47	44
Anterior	0.51	48
Lateral	0.28	26
Posterior	0.43	46

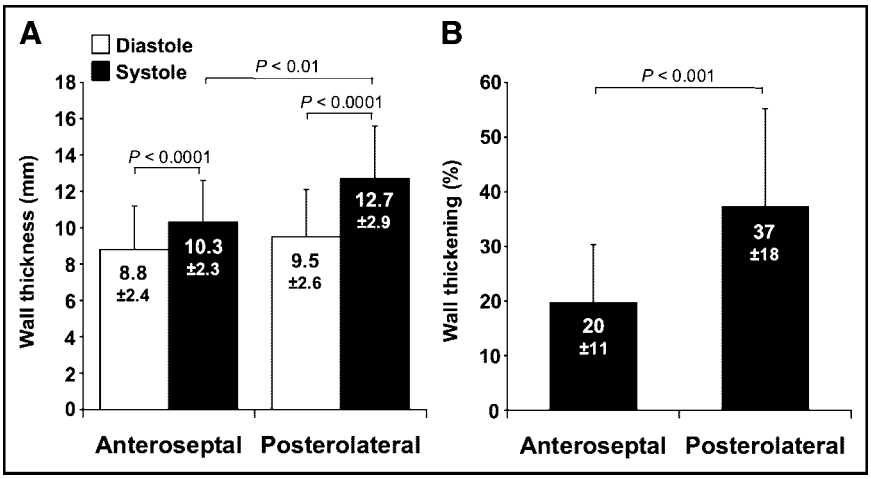

FIGURE 2. End-diastolic (diastole) and end-systolic (systole) wall thickness (A) and systolic wall thickening in percentage of the anteroseptal and posterolateral wall (B) in 14 patients with LBBB without coronary artery disease. Values were determined from parasternal echocardiographic M-mode recordings.

pattern of the left ventricle ($P < 0.0001$; Fig. 1C). In analogy to the distribution pattern of relative ^{99m}Tc-MIBI uptake, wall thickening was highest in the lateral wall (55% ± 17%, $P < 0.0001$ compared with the remaining wall areas) and lowest in the septum (16% ± 14%).

These findings were substantiated by the echocardiographic M-mode measurements, which demonstrated a comparable regional difference in wall thickening for the corresponding anteroseptal and posterolateral walls (Fig. 2).

DISCUSSION

It is a well-known phenomenon that patients with complete LBBB exhibit a heterogeneous distribution pattern of myocardial perfusion as estimated with ^{201}Tl or ^{99m}Tc-MIBI SPECT. Stress-induced septal hypoperfusion is frequently observed, but diminished septal perfusion, compared with the lateral free wall, also occurs in resting studies even in the absence of coronary artery disease (*1,2*). Downregulated perfusion secondary to diminished oxygen demand, increased intramyocardial pressure during diastole, fibrotic alterations, or pronounced partial-volume effects due to reduced wall thickening have been discussed as the pathophysiologic correlates of these observations (*3,14–17*).

Partial-volume effects are of particular relevance in myocardial SPECT studies. Because of the limited spatial resolution of γ-cameras, systolic thickening and diastolic relaxation of the myocardium entail continuous changes in the recovery coefficient during acquisition. Therefore, the myocardial counts actually measured depend considerably on systolic thickening, as marked thickening leads to a higher recovery coefficient and subsequently to more myocardial counts.

The main findings of our study are that, in patients with dilated cardiomyopathy and LBBB, resting MBF and its LV distribution pattern as estimated with the partial-volume–independent method of ^{15}O-water PET are within the range of values observed in healthy controls, without evidence of regional heterogeneity (*18*). However, ^{99m}Tc-MIBI uptake and wall thickening as estimated by gated ^{18}F-FDG PET differ significantly between the respective wall areas in an identical pattern. This finding was confirmed by M-mode echocardiography from corresponding regions.

There is further evidence of regional heterogeneity in systolic shortening and myocardial wall thickness in patients with asynchronous electrical activation of the left ventricle. In animal experiments during ventricular pacing, regional systolic shortening proved to be reduced in early-activated regions and increased in late-activated regions as determined with MRI tagging (*19*). These data could recently be confirmed by echocardiographic strain rate imaging in humans with complete LBBB, whose interventricular septum represents the early-activated region and the lateral free wall the late-activated region (*20*). The reduction of ^{99m}Tc-MIBI uptake in the anterior and posterior wall in our patients must also be interpreted as resulting from a relative reduction in regional wall thickening compared with the lateral wall. This reduction in wall thickening occurred mainly in the adjacent anteroseptal and posteroseptal parts of the anterior and posterior walls, respectively.

Furthermore, diminished end-diastolic wall thickness of the septum, compared with the late-activated posterior wall, has been described in LBBB, whereas end-diastolic wall thickness was identical in both wall areas in healthy controls (*21*). In our echocardiography analysis, we could verify a trend of smaller end-diastolic wall thickness in the anteroseptal wall compared with the posterolateral wall, which, however, did not reach statistical significance.

Therefore, at least one of these alterations in LBBB, namely reduced systolic thickening and diminished end-diastolic wall thickness in the septum and adjacent anteroseptal and posteroseptal walls, provides a pathophysiologic explanation for the heterogeneous uptake pattern in resting ^{201}Tl or ^{99m}Tc-MIBI SPECT studies due to pronounced partial-volume effects.

Our results argue against the concept of downregulated septal perfusion caused by diminished oxygen demand, as MBF was found to be similar in all myocardial regions by ^{15}O-water PET. This finding is underscored by data of

Zanco et al., who, using ^{13}N-NH_3 PET, found preserved septal perfusion in patients with LBBB and reduced LV function but without coronary artery disease (*22*).

It is unlikely that the variability in the ^{15}O-water measurements influenced our results. Calculation of repeatability coefficients from our data revealed good agreement of both measurements in each patient. The repeatability coefficients of our parameters were almost identical to previously published values obtained in similar settings (*6*,*23*).

CONCLUSION

^{15}O-Water PET proves that resting MBF is homogeneously distributed in patients with nonischemic dilated cardiomyopathy and LBBB. The quantitative analysis of ^{99m}Tc-MIBI SPECT in these patients is significantly affected by heterogeneity in regional myocardial systolic wall thickening. Therefore, supplementary analysis and consideration of wall thickening derived from ECG-gated data is recommended in the assessment of ^{99m}Tc-MIBI SPECT in patients with LBBB. The reader should take into account that the combination of reduced septal ^{99m}Tc-MIBI uptake and reduced septal wall thickening does not necessarily represent myocardial infarction, as this combination usually occurs in patients without LV conduction disturbances (*24*). Reduced septal ^{99m}Tc-MIBI uptake should rather be considered the artificial result of reduced wall thickening.

REFERENCES

1. Altehoefer C, vom Dahl J, Kleinhans E, Uebis R, Hanrath P, Buell U. 99Tcm-methoxyisobutylisonitrile stress/rest SPECT in patients with constant complete left bundle branch block. *Nucl Med Commun.* 1993;14:30–35.
2. Lebtahi NE, Stauffer JC, Delaloye AB. Left bundle branch block and coronary artery disease: accuracy of dipyridamole thallium-201 single-photon emission computed tomography in patients with exercise anteroseptal perfusion defects. *J Nucl Cardiol.* 1997;4:266–273.
3. Sugihara H, Tamaki N, Nozawa M, et al. Septal perfusion and wall thickening in patients with left bundle branch block assessed by technetium-99m-sestamibi gated tomography. *J Nucl Med.* 1997;38:545–547.
4. Iida H, Kanno I, Takahashi A, et al. Measurement of absolute myocardial blood flow with $H_2{}^{15}O$ and dynamic positron-emission tomography: strategy for quantification in relation to the partial-volume effect. *Circulation.* 1988;78:104–115.
5. Iida H, Rhodes CG, de Silva R, et al. Myocardial tissue fraction-correction for partial volume effects and measure of tissue viability. *J Nucl Med.* 1991;32:2169–2175.
6. Wyss CA, Koepfli P, Mikolajczyk K, Burger C, von Schulthess GK, Kaufmann PA. Bicycle exercise stress in PET for assessment of coronary flow reserve: repeatability and comparison with adenosine stress. *J Nucl Med.* 2003;44:146–154.
7. Iida H, Rhodes CG, de Silva R, et al. Use of the left ventricular time-activity curve as a noninvasive input function in dynamic oxygen-15-water positron emission tomography. *J Nucl Med.* 1992;33:1669–1677.
8. Hove JD, Gambhir SS, Kofoed KF, Freiberg J, Kelbæk H. Quantitation of the regional blood flow in the interventricular septum using positron emission tomography and nitrogen-13 ammonia. *Eur J Nucl Med Mol Imaging.* 2003;30:109–116.
9. Kety S. Measurement of local blood flow by the exchange of an inert, diffusible substance. *Methods Med Res.* 1960;8:228–236.
10. Bland JM, Altman DG. Statistical methods for assessing agreement between two methods of clinical measurement. *Lancet.* 1986;327:307–310.
11. *Precision of Test Methods I: Guide for the Determination and Reproducibility for a Standard Test Method.* London, U.K.: British Standards Institution; 1976:54–97.
12. Kupferschlager J, Muller B, Schulz G, et al. A method for combined scatter and attenuation correction without transmission measurement for myocardial SPECT with 99m-Tc binding. *Nuklearmedizin.* 1997;36:56–64.
13. Schaefer WM, Lipke C, Nowak B, et al. Validation of an evaluation routine for left ventricular volumes, ejection fraction and wall motion from gated cardiac FDG PET: a comparison with cardiac magnetic resonance imaging. *Eur J Nucl Med Mol Imaging.* 2003;30:545–553.
14. Burns RJ, Galligan L, Wright LM, Lawand S, Burke RJ, Gladstone PJ. Improved specificity of myocardial thallium-201 single-photon emission computed tomography in patients with left bundle branch block by dipyridamole. *Am J Cardiol.* 1991;68:504–508.
15. Ono S, Nohara R, Kambara H, Okuda K, Kawai C. Regional myocardial perfusion and glucose metabolism in experimental left bundle branch block. *Circulation.* 1992;85:1125–1131.
16. Carew TE, Covell JW. Effect of intramyocardial pressure on the phasic flow in the interventricular septal artery. *Cardiovasc Res.* 1976;10:56–64.
17. Wackers FJ. Myocardial perfusion defects in left bundle branch block: true or false? Fact or artifact? *J Nucl Cardiol.* 1997;4:550–552.
18. Chareonthaitawee P, Kaufmann PA, Rimoldi O, Camici PG. Heterogeneity of resting and hyperemic myocardial blood flow in healthy humans. *Cardiovasc Res.* 2001;50:151–161.
19. Prinzen FW, Hunter WC, Wyman BT, McVeigh ER. Mapping of regional myocardial strain and work during ventricular pacing: experimental study using magnetic resonance imaging tagging. *J Am Coll Cardiol.* 1999;33:1735–1742.
20. Breithardt OA, Stellbrink C, Herbots L, et al. Cardiac resynchronization therapy can reverse abnormal myocardial strain distribution in patients with heart failure and left bundle branch block. *J Am Coll Cardiol.* 2003;42:486–494.
21. Prinzen FW, Cheriex EC, Delhaas T, et al. Asymmetric thickness of the left ventricular wall resulting from asynchronous electric activation: a study in dogs with ventricular pacing and in patients with left bundle branch block. *Am Heart J.* 1995;130:1045–1053.
22. Zanco P, Desideri A, Mobilia G, et al. Effects of left bundle branch block on myocardial FDG PET in patients without significant coronary artery stenoses. *J Nucl Med.* 2000;41:973–977.
23. Kaufmann PA, Gnecchi-Ruscone T, Yap JT, Rimoldi O, Camici PG. Assessment of the reproducibility of baseline and hyperemic myocardial blood flow measurements with ^{15}O-labeled water and PET. *J Nucl Med.* 1999;40:1848–1856.
24. DePuey EG, Rozanski A. Using gated technetium-99m-sestamibi SPECT to characterize fixed myocardial defects as infarct or artifact. *J Nucl Med.* 1995;36:952–955.